Bangladesh J. Bot. **48**(3): 427-436, 2019 (September)

A GREEN APPROACH FOR THE BIOSYNTHESIS OF POWDERED SILVER NANOPARTICLES USING LEAF EXTRACT OF *TRIGONELLA FOENUM-GRAECUM* L.: CHARACTERIZATION AND ANTIBACTERIAL EVALUATION

T RAJKUMAR AND JAYANTA KUMAR PATRA*[1]

University of Szeged, Interdisciplinary Excellence Centre, Department of Applied and Environmental Chemistry, H-6720, Rerrich Béla tér 1, Szeged, Hungary

Key words: Green synthesis, Silver nanoparticles, *Trigonella foenum-graecum*, X-ray diffraction, Antibacterial evaluation

Abstract

Silver nanoparticles (AgNPs) were synthesized using aqueous leaf extract of *Trigonella foenum-graecum* as reducing and stabilizing agent. The ultraviolet-visible spectrum showed absorption peak at 480 nm. XRD pattern indicates the formation of face-centered cubic structure of silver nanoparticles. FESEM images indicate the presence of spherical silver nanoparticles with the particle size of ~90 nm. FTIR indicates that the participation of different functional groups present in the biomolecules is responsible for both reducing and stabilizing the formation of nanoparticles. The synthesized AgNPs demonstrated positive antibacterial activity against two different foodborne pathogenic bacteria (*Escherichia coli* O157:H7 ATCC 35150, *Staphylococcus aureus* ATCC 13565) with zones of inhibition of 9.20 ± 0.18 and 9.34 ± 0.11, respectively and MIC and MBC of 100 and >100 µg/ml, respectively. The synthesized AgNPs could serve as a candidate for development of antibacterial drugs or additive in the food packaging system for its application in medicine, cosmetics and food sector industries.

Introduction

In recent years, silver nanoparticles (AgNPs) were studied due to their catalytic (Vidhu and Philip 2014), electronic (McConnell *et al.* 2000), optical properties (Kassab *et al.* 2016) and their significant antimicrobial activities (Ahmed *et al.* 2015, Bindhu and Umadevi 2015 and Ghaedi *et al.* 2015). Size and shape of AgNPs determine its antibacterial activity (Pal *et al.* 2007). The proposed mechanism of antibacterial effect of AgNPs is the damage of the bacterial cell wall and consequently disturbing their enzymatic activities (Ahmed *et al.* 2016). Various methods have been adopted for the preparation of AgNPs that includes physical methods (microwave radiation, ultrasonic radiation, UV radiation and laser radiation) (Arvizo *et al.* 2012), chemical methods (chemical reduction and electrochemical synthesis) (Yang *et al.* 2010) and biological methods using microorganisms (Du and Yi 2010) and plant extracts (Li *et al.* 2007, Karuppiah and Rajmohan 2013, Kumar *et al.* 2014, Ghaedi *et al.* 2015 and Rajaram *et al.* 2015). Among these methods, chemical reduction was used extensively because it is simple, shape and size can be controlled easily by varying the pH of the medium. However, this method uses hazardous reducing agents such as sodium borohydride and sodium citrate which may cause serious environmental pollution. Hence, preparation of AgNPs using environmentally friendly method is desirable. Various approaches have been used especially using microorganisms and plant extracts, but microorganism mediated synthesis needs tedious process of cell culture. Plant extract mediated synthesis was proved to be environmentally friendly and biocompatible as it does not require any hazardous chemicals. Various plant extracts were utilized for the preparation of AgNPs (Iravani 2011). Plant extract contains various phytochemicals which contributes to the reduction and stabilization of silver nanoparticles (Moniruzzaman *et al.* 2015).

*Author for correspondence: <jkpatra@dongguk.edu>. [1]Research Institute of Biotechnology & Medical Converged Science, Dongguk University-Seoul, Gyeonggi-do 10326, Republic of Korea.

With the occurrence of a number of multiple resistant microorganisms to various antibiotics, there is an imperative necessity for development of strong and new antimicrobial agents to tackle these disease-causing microbes. Many studies have highlighted the potential applications of metal nanoparticles as antimicrobial drugs (Gade *et al.* 2008 and Patra and Baek 2016). Nowadays, the use of silver nanoparticles as antimicrobial drugs has been increasing due to its potent antimicrobial properties together with the catalytic and high surface to volume ratios properties (Rai *et al.* 2014, Yahyaei *et al.* 2014 and Patra and Baek 2016). Currently, AgNPs is used in medicine and related applications (Patra and Baek 2016 and Mukherjee *et al.* 2008).

Trigonella foenum-graecum is an annual plant belongs to the family Fabaceae and cultivated in different parts of the world (Sadeghzadeh-Ahari *et al.* 2010). Its seeds and leaves are used as ingredients in dishes in different parts of the world (Acharya *et al.* 2006). The main constituents are flavonoids, alkaloids, vitamins and amino acids (Albasha and El-Saied Azad 2014 and Hasona *et al.* 2016).

The biosynthesis of AgNPs by green synthesis method using the ecofriendly, non-toxic and cost effective *Trigonella foenum-graecum* extract as the reducing agents followed by its characterization is reported. The antibacterial activity of AgNPs was studied against the dreadful food borne pathogenic bacteria such as *Escherichia coli* O157:H7 ATCC 35150 and *Staphylococcus aureus* ATCC 13565.

Materials and Methods

Silver nitrate ($AgNO_3$, Analytical Reagent grade) was purchased from S.D. fine chemical Ltd. (Mumbai, India). Dried leaves of *Trigonella foenum-graecum* were purchased from local market Chennai, Tamilnadu, India during July 2017. Dried leaves of *Trigonella foenum-graecum* were washed thoroughly with tap water and then washed twice with distilled water and ground with mortar and pestle. One gram of the powdered leaves was taken in a round bottom flask fitted with water condenser and boiled for 30 min using 100 ml of double distilled water. It was cooled and filtered with Whatman No. 1 filter paper. The extract was kept in refrigerator for future use.

For the synthesis of silver nanoparticles (AgNPs), 10 ml of the leaf extract was mixed with 100 ml of 1 mM silver nitrate solution and heated in a water bath, set at 80°C for 5 min (Raja *et al.* 2017). Change of colour from yellow to dark brown indicates the colloidal AgNPs formation.

Ultraviolet-visible spectrum was measured on a Shimadzu-2450 UV-vis spectrophotometer operating in the range 200-800 nm. The FTIR spectrum of dried leaf extract and nanoparticle powder was obtained with Jasco FT-IR 6300 spectrometer using KBr pellet method at a resolution of 4/cm. SEM investigations were performed using Zeiss Field emission scanning electron microscope. XRD (X'Pert MRD, PANalytical, Almelo, The Netherlands) of the AgNPs was measured at the operating voltage of 30 kV and current of 40 mA. Cu Kα radiation was used at an angle of 2θ from 10° to 90° in 0.01 steps at a scan speed of 10°/min.

The antibacterial prospective of AgNPs was determined against three different foodborne pathogenic bacteria by the standard disc diffusion method (Patra and Baek 2016). Three pathogenic bacteria (*Escherichia coli* O157:H7 ATCC 35150, *Staphylococcus aureus* ATCC 13565 and *Pseudomonas aeruginosa* ATCC 27583) were procured from ATCC, Manassas, VA, USA and streak plated in fresh nutrient agar (NA) plates for 24 hrs at 37°C. Later, only 2-3 well isolated colonies were collected using an inoculating loop and put into freshly prepared nutrient broth (NB) media and sub-cultured. Prior to use, the OD value of the cultured bacteria were recorded at 600 nm and the concentration of the bacterial cells were maintained at 1.5×10^8 CFU/ml in order to maintain the standard turbidity of the bacterial cells. The culture bacteria were immediately taken for the antibacterial experiment. Solutions of powdered AgNPs were made at a

concentration of 1,000 µg/ml in 5% dimethylsulphoxide (DMSO) with a sonication for 15 min at 30°C to prepare a colloidal solution. Two different concentrations (50 and 100 µg AgNPs/disc) of paper discs were prepared for the antibacterial screening. The AgNPs impregnated paper discs were placed on the nutrient agar (NA) plates that were previously uniformly spreaded with overnight grown pathogen cultures in NB media (1×10^7 CFU/ml). The plates were then incubated at 37°C for 24 hrs. The antibacterial activity of the AgNPs were calculated in terms of their diameters of the zones of inhibition around each paper disc. Antibiotic, gentamycin (10 µg/disc) was taken as positive control and 5% DMSO was taken as the negative control for the antibacterial experiment. All the tests were carried out in triplicates.

The minimum inhibitory concentration (MIC) and minimum bactericidal concentration (MBC) of the synthesized AgNPs against the three foodborne pathogenic bacteria were determined by the two-fold dilution method, with minor modifications (Patra and Baek 2016). Prior to use, different dilutions of the AgNPs in 5% DMSO (100, 50 and 25 µg/ml) were prepared by two-folds dilution method in NB in a 96 well microplate and to them, 10 µl of the overnight grown culture of each bacterial strain was inoculated separately. The samples were then incubated at 37°C for 24 hrs. The lowest concentration of AgNPs with no visible growth of the tested bacteria was determined to be the MIC value in µg/ml whereas the lowest concentration that displayed complete absence of the bacterial colonies growth on the surface of NA plates was designated as the MBC value in µg/ml.

Results and Discussion

AgNPs formation was observed by colour change and ultraviolet-visible spectroscopy. The colour of the aqueous solution of silver nitrate was changed from pale yellow to dark brown following by the addition of leaf extract that indicated the formation of AgNPs. It is well known that $AgNO_3$ can be reduced to metallic silver by various phytochemicals exist in the leaf extract (Moldovan *et al.* 2016). The colour is due to the characteristic Surface Plasmon Resonance (SPR) of the silver nanoparticles (Rycenga *et al.* 2011). UV-visible spectra of the solution showed a strong absorption peak centered around 480 nm which is the characteristic surface SPR of spherical AgNPs (Raghunandan *et al.* 2011, Donda *et al.* 2013 and Gupta *et al.* 2014). The position of SPR depends on various factors such as size, shape and particles formed (Mulvaney 1996). The reduction of silver ions was completed in 2 hrs. After 2 hrs, there is no change in the intensity of the peak.

The UV-visible spectra of AgNPs formation using silver nitrate concentrations between 0.5 and 3 mM are shown in Fig. 1A. The SPR band intensity increases with increase in the concentration of silver nitrate from 0.5mM to 2.25 mM. On further increase in concentration of silver nitrate from 2.25 to 3 mM, the SPR band intensity decreases. The optimum SPR peak intensity was obtained at 2.25 mM of $AgNO_3$. These results agree with those reported by Ibrahim who prepared AgNPs using banana peel extract and found that the maximum SPR peak intensity was observed at 1.75 mM silver nitrate concentration and on further increasing the concentration the SPR band intensity decreases (Ibrahim 2015).

Fig. 1B shows the UV-Visible spectra of AgNPs obtained with changing the concentration of leaf extract from 1 ml to 5 ml keeping silver nitrate concentration (2.25 mM) constant. The maximum SPR peak intensity was observed for 1 ml extract. It has been observed that increase in the concentration of leaf extract, i.e. 2 ml, the formation of AgNPs was less. However, on further increase in the concentration of leaf extract from 3ml to 5 ml there is no formation of AgNPs. This is probably due to the complete saturation of the silver ions surface by the phytochemicals present in the extract. Similar results were also reported in the literature (Matos *et al.* 2011).

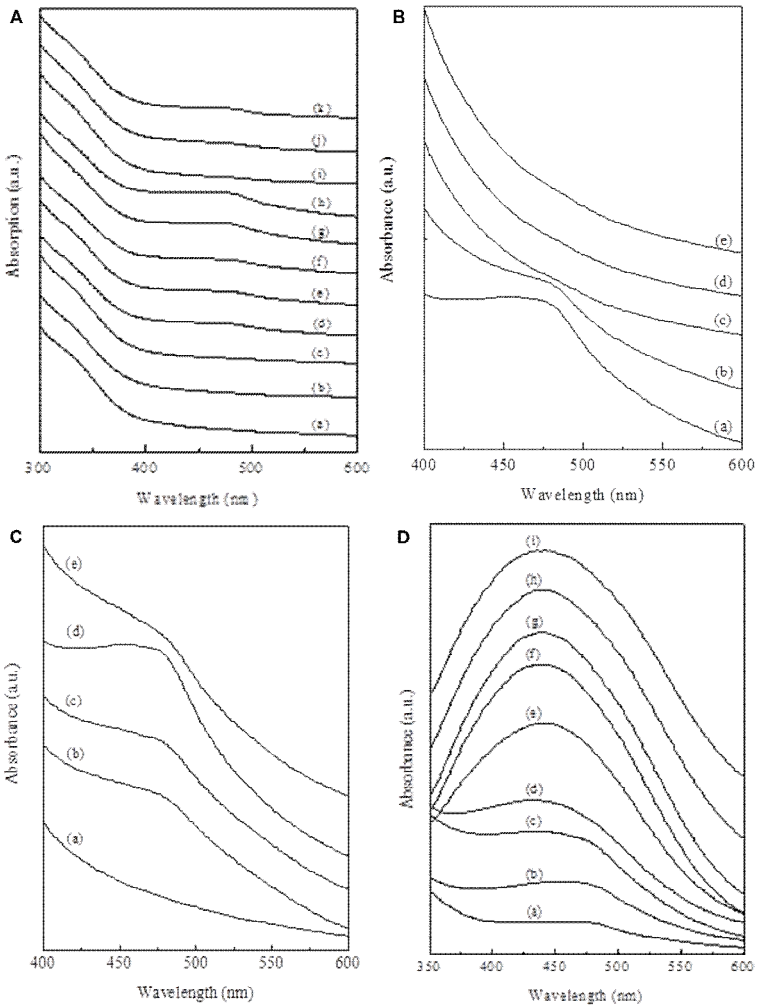

Fig. 1 (A). UV-vis absorption spectra of AgNPs prepared with $AgNO_3$ concentrations of (a) 0.5 mM, (b) 0.75 mM, (c) 1 mM, (d) 1.25 mM, (e) 1.5 mM, (f) 1.75 mM, (g) 2 mM, (h) 2.25 mM, (i) 2.5 mM, (j) 2.75 mM, (k) 3 mM using 1 ml of leaf extract at 100°C. (B) UV-vis absorption spectra of AgNPs prepared at different concentrations of leaf extract and 2.25 mM $AgNO_3$ at 100°C, (a) 1 ml leaf extract, (b) 2 ml leaf extract, (c) 3 ml leaf extract, (d) 4 ml leaf extract, (e) 5 ml leaf extract; (C) UV–vis absorption spectra of AgNPs prepared at different temperatures using 1ml of leaf extract and 2.25mM $AgNO_3$, (a) 40°C, (b) 60°C, (c) 80°C, (d) 100°C, (e) 120°C, (D) Fig. 4 UV-vis absorption spectra of AgNPs prepared at different time using 1ml of leaf extract and 2.25 mM $AgNO_3$ at 100 °C, (a) 5 min, (b) 10 min, (c) 20 min, (d) 30 min, (e) 1 hr, (f) 2 hrs, (g) 3 hrs, (h) 4 hrs and (i) 5 hrs.

Fig. 1C shows the UV-visible spectra of AgNPs obtained at different temperatures in the range of 40-120°C. Formation of AgNPs was increased with the rise in temperature. As the temperature is increased the absorption maximum slightly blue shifted from 480 to 479 nm. This indicates that the size of the nanoparticles decreases with increasing temperature. This is in complete agreement with the study reported previously (Verma and Mehata 2016).

Fig. 1D shows the UV-Visible spectra of AgNPs obtained at different reaction time intervals. The rate of silver ions reduction increases slowly up to 30 min. After 30 min, the rate of reduction was fast. The maximum reduction of silver ions was obtained at 2 hrs. After 2 hrs, the rate of reduction was constant. As the time is increased the absorption maximum slightly blue shifted from 480 to 440 nm. This indicates that particle size decreases with time. The increase in intensity with time can be ascribed to increased formation of silver nanoparticles (Joseph and Mathew 2015). The broad absorption peak indicates broad particle size distribution (Zayed *et al.* 2012).

Crystal structure of AgNPs was studied by XRD. The XRD pattern of the AgNPs is shown in Fig 2A. The XRD pattern showed intense peaks at $2\theta = 38^{o}$, 44^{o}, 64^{o} and 77^{o} is due to (111), (200), (220) and (311) crystal planes of face-centered cubic AgNPs (JCPDS file No. 04-0783). The most intense peak at $2\theta = 32°$ may be due to the presence of mixed phase of Ag/Ag_2O (Firdhouse and Lalitha 2016). The additional peaks observed can be attributed to the crystallization of bioorganic phases that is attached on the surface of the nanoparticles. This observation is well in agreement with previous report (Kumara *et al.* 2012, Ahluwalia *et al.* 2014, Goudarzi *et al.* 2016, Patra and Baek 2016). Size, shape and morphology of the AgNPs was studied by Scanning Electron Microscopy. Fig. 2B shows SEM images of the AgNPs. SEM studies showed highly aggregated spherical AgNPs (Govindaranjan *et al.* 2016). The average particle size was ~ 90 nm. Fig. 2C shows FTIR spectra of dried *Trigonella foenum-graecum* leaf extract and synthesized AgNPs. FTIR analysis of dried *Trigonella foenum-graecum* leaf extract revealed bands at 3424, 2933, 2169, 1614, 1394, 1114, 620 cm^{-1}. The band at 3424 cm^{-1} corresponds to O-H and N-H stretching vibrations (Sriranjani *et al.* 2016). Less intense peak at 2933 cm^{-1} is due to C-H stretching vibration of methylene groups of protein (Bar *et al.* 2009, Ganesh Kumar and Mamidyala 2011). The band at 1614 cm^{-1} corresponds to (NH) C=O stretching vibration (amide I band) of protein (Bar *et al.* 2009). The band at 1394 cm^{-1} is due to C-H stretching vibration (Thatoi *et al.* 2016). The band at 620 cm^{-1} can be attributed to C-H bend of alkynes (Rastogi and Arunachalam 2011). FTIR spectra of synthesized AgNPs show band at 3424, 2923, 1610, 1398, 1184, 632 cm^{-1}. The slight shifting of IR peaks between AgNPs and *Trigonella foenum-graecum* leaf extract indicates the involvement of these functional groups as reducing and stabilizing agents (Thatoi *et al.* 2016).

The results of the antibacterial activity of synthesized AgNPs against the three foodborne pathogenic bacteria is presented in Table 1. AgNPs at 100 µg/disc were active against *E. coli* O157:H7 and *S. aureus* with 9.20 and 9.34 mm diameter of inhibition zone respectively, however it was not active against *P. aeruginosa* at any of the tested concentrations. The standard positive control, kanamycin exhibited diameter of zones of inhibition ranged between 10.95 and 11.65 mm (Table 1) at 10 µg/disc. The negative control didn't show any positive activity against all the three tested bacteria. The MIC values was found out to be 100 µg/ml, and the MBC values were found to be >100 µg/ml against both the positive bacteria (Table 1).

Since time immoral, the silver metal has been used for a variety of purposes with potential applications including antimicrobial potentials (Nakkala *et al.* 2014, Ali *et al.* 2016). In the present study, the synthesized AgNPs indicated a broad spectrum of antibacterial action against the tested bacteria that might have been caused due to the differences in the morphological structures of each bacteria. From the results, it is evident that the synthesized AgNPs exhibited moderate antibacterial activity against the tested pathogens, however if they are treated in formulations or in combination with antibiotics, their activity will increase as a result of the synergistic effects and the use of chemical components could be minimized. Various literature have suggested that as compared to AgNPs alone the combination of antibiotic with the AgNPs will be able to release Ag^{+} at a higher rate and thus the antibacterial activity will be enhanced (Katva *et al.* 2017).

Table 1. Antibacterial activity, MIC and MBC of AgNPs against three different foodborne pathogenic bacteria.

Pathogenic bacteria	Diameter of zones of inhibition in mm		Positive control	Negative control	MIC in µg/ml	MBC in µg/ml
	50 µg/disc	100 µg/disc	10 µg/disc			
E. coli O157:H7 ATCC 35150	0 ± 0	9.20 ± 0.18*	11.65 ± 0.60*	0 ± 0	100	>100
S. aureus ATCC 13565	0 ± 0	9.34 ± 0.11*	10.95 ± 0.47*	0 ± 0	100	>100
P. aeruginosa ATCC 27583	0 ± 0	0 ± 0	11.33 ± 0.33*	0 ± 0	-	-

*values are expressed as the mean value of three independent replications with standard deviation; - : Not detected; > : Value is greater than; positive control: Gentamycin; negative control: 5% DMSO.

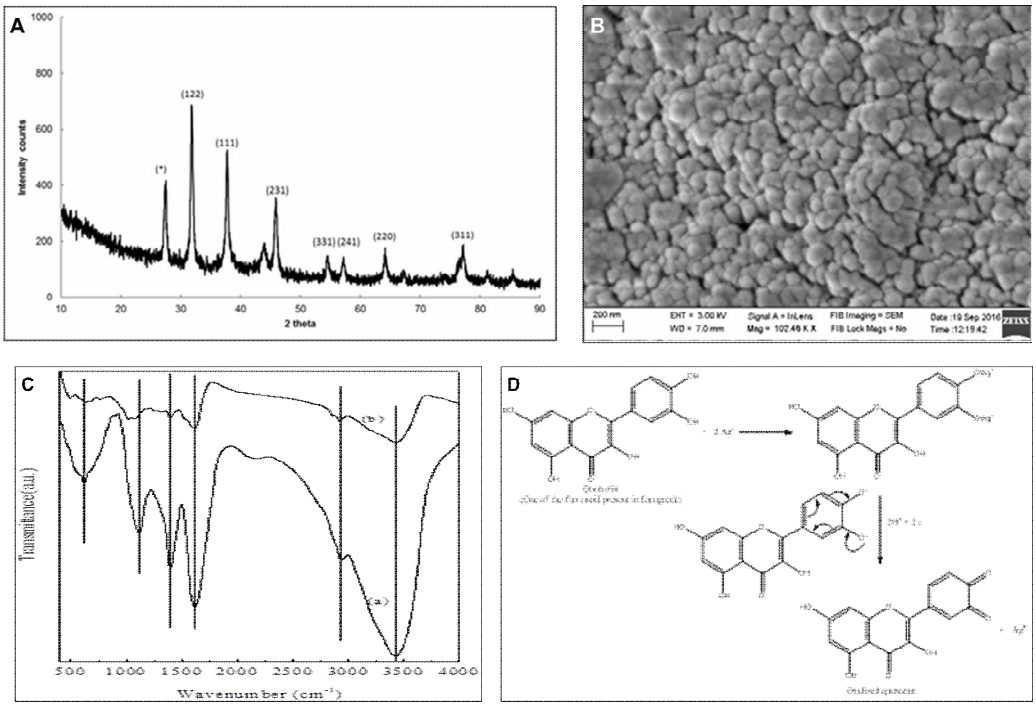

Fig. 2(A). XRD pattern of biosynthesized AgNPs using 1 ml of leaf extract and 2.25 mM $AgNO_3$ at 100°C for a time duration of 2 hrs; (B) FESEM image of AgNPs; (C) FTIR spectra of (a) pure leaf extract, (b) Silver nanoparticles; (D) The possible mechanism for the formation of bio-reduced AgNPs.

Though the mechanism of action of AgNP is uncertain in case of the microorganisms (Kim *et al.* 2011); however, it is presumed that the AgNPs due to its reduced size, might have entered inside the cells of the bacteria and could have diminished its respiration process due to diminution of the energy compounds or by triggering cell membrane damage (Swamy *et al.* 2015 and Patra and Baek 2016).

The exact mechanism for the formation of silver nanoparticle using plant extract is not known. According to the previous literature (Shukla *et al.* 2008, Iravani 2011), the presence of polyphenoloic/alcoholic compounds, flavonoids, aldehydes/ketones and proteins are responsible

for the reduction of $AgNO_3$ to silver nanoparticles and their stabilization. The plausible mechanism is given in Fig. 2D. Fig. 2D, describes that the flavonoid compounds (possibly the quercetin) present in the aqueous leaf extract of *Trigonella foenum-graecum* might act as the reducing agent and react with the silver ions from the $AgNO_3$ solution and form the stabilized AgNPs. The flavonoid compounds (possibly the quercetin) also might have acted as the stabilizing agents in the synthesis process.

Green synthesis of AgNPs was carried out using aqueous leaf extract of *Trigonella foenum-graecum*. This process is cost effective, ecofriendly and alternative approach to conventional physical and chemical methods. In this method, highly crystalline, spherical shaped AgNPs are formed. The biomolecules present in the leaf extract were responsible for both reduction and stabilization of AgNPs. The synthesized AgNPs showed promising antibacterial activity against *Escherichia coli* O157:H7 ATCC 35150 and *Staphylococcus aureus* ATCC 13565. This antibacterial potential can be used for development of antibacterial drugs and food packaging system to be applicable in food and pharmaceutical industries.

Acknowledgements

The authors like to acknowledge the FESEM facilities provided by UGC-DAE, Kalpakkam. The research is also supported by Dongguk University research fund for the year 2016-2018.

References

Ahluwalia V, Kumar J, Sisodia R, Shakil NA and Walia S 2014. Green synthesis of silver nanoparticles by *Trichoderma harzianum* and their bio-efficacy evaluation against *Staphylococcus aureus* and *Klebsiella pneumonia*. Ind. Crops. Prod. **55**: 202-206.

Ahmed MJ, Murtaza G, Mehmood A and Bhatti TM 2015. Green synthesis of silver nanoparticles using leaves extract of *Skimmia laureola*: Characterization and antibacterial activity. Mater. Lett. **153**: 10-13.

Ahmed S, Ahmad M, Swami BL and Ikram S 2016. A review on plants extract mediated synthesis of silver nanoparticles for antimicrobial applications: A green expertise. J. Adv. Res. **7**: 17-28.

Albasha MO and El-Saied Azab A 2014. Effect of cadmium on the liver and amelioration by aqueous extracts of fenugreek seeds, rosemary, and cinnamon in guinea pigs: Histological and biochemical study. Cell Biol. **2**: 7-17.

Ali M, Kim B, Belfield KD, Norman D, Brennan M and Ali GS 2016. Green synthesis and characterization of silver nanoparticles using *Artemisia absinthium* aqueous extract - A comprehensive study. Mater. Sci. Eng. C. **58**: 359-365.

Arvizo RR, Bhattacharyya S, Kudgus RA, Giri K, Bhattacharya R and Mukherjee P 2012. Intrinsic therapeutic applications of noble metal nanoparticles: past, present and future. Chem. Soc. Rev. **41**: 2943-2970.

Bar H, Bhui DK, Sahoo GP, Sarkar P, De SP and Misra A 2009. A green synthesis of silver nanoparticles using latex of *Jatropha curcas*. Colloids and Surf. A. **339**: 134-139.

Bindhu MR and Umadevi M. 2015. Antibacterial and catalytic activities of green synthesized silver nanoparticles. Spetrochim. Acta. A. **135**: 373-378.

Donda MR, Kudle KR, Alwala J, Miryala A, Sreedhar B and Pratap Rudra MP 2013. Synthesis of silver nanoparticles using extracts of *Securinega leucopyrus* and evaluation of its antibacterial activity. Int. J. Curr. Sci. **7**: 1-8.

Du J and Yi TH 2016. Biosynthesis of silver nanoparticles by *Variovorax guangxiensis* THG-SQL3 and their antimicrobial potential. Mater. Lett. **178**: 75-78.

Firdhouse MJ and Lalitha P 2016. Biogenic silver nanoparticles - Synthesis, characterization and its potential against cancer inducing bacteria. J. Mol. Liq. **222**: 1041-1050.

Gade, AK, Bonde P, Ingle AP, Marcato PD, Duran N and Rai MK 2008. Exploitation of *Aspergillus niger* for synthesis of silver nanoparticles. J. Biobased. Mater. Bio. **2**: 243-247.

Ganesh Kumar C and Mamidyala SK 2011. Extracellular synthesis of silver nanoparticles using culture supernatant of *Pseudomonas aeruginosa*. Colloids Surf. B. **84**: 462-466.

Ghaedi M, Yousefinejad M, Safarpoor M, Zare Khafri H and Purkait MK 2015. Rosmarinus officinalis leaf extract mediated green synthesis of silver nanoparticles and investigation of its antimicrobial properties. J. Ind. Eng. Chem. **31**: 167-172.

Goudarzi M, Mir N, Mousavi-Kamazani M, Bagheri S and Salavati-Niasari M 2016. Biosynthesis and characterization of silver nanoparticles prepared from two novel natural precursors by facile thermal decomposition methods. Scientific Report. **6**: 32539, DOI: 10.1038/srep32539

Govindarajan M, Vijayan P, Kadaikunnan S, Alharbi NS and Benelli G 2016. One-pot biogenic fabrication of silver nanocrystals using *Quisqualis indica*: Effectiveness on malaria and Zika virus mosquito vectors, and impact on non-target aquatic organisms. J. Photoch. Photobio. B. **162**: 646-655.

Gupta K, Hazarika SN, Saikia D, Namsa ND and Mandal M 2014. One step green synthesis and anti-microbial and anti-biofilm properties of *Psidium guajava* L. leaf extract-mediated silver nanoparticles. Mater. Lett. **125**: 67-70.

Hasona NA, Ahmed MQ, Alghassab TA, Alghassab MA and Alghabban AA 2016. Antihyperlipidemic effect of pomegranate peel and Iranian fenugreek extracts on cholesterol-rich diet-induced hyperchole sterolemia in guinea pigs. Merit Res. J. Med. Med. Sci. **4**: 196-203.

Ibrahim HMM 2015. Green synthesis and characterization of silver nanoparticles using banana peel extract and their antimicrobial activity against representative microorganisms. J. Radiat. Res. Appl. Sci. **8**: 265-275.

Iravani S 2011. Green synthesis of metal nanoparticles using plants. Green Chem. 10: 2638-2650.

Joseph S and Mathew B 2015. Microwave assisted facile green synthesis of silver and gold nanocatalysts using the leaf extract of *Aerva lanata*. Spectrochim. Acta A. **136**: 1371–1379.

Karuppiah M and Rajmohan R 2013. Green synthesis of silver nanoparticles using *Ixora coccinea* leaves extract. Mater. Lett. **97**: 141-143.

Kassab LRP, Silva DM, Garcia JAM, da Silva DS and de Araujo CB 2016. Silver nanoparticles enhanced photoluminescence of Nd3+ doped germanate glasses at 1064 nm, Opt. Mater. **60**: 25-29.

Katva S, Das S, Singh Moti H, Jyoti A and Kaushik S. 2017. Antibacterial synergy of silver nanoparticles with gentamicin and chloramphenicol against *Enterococcus faecalis*. Pharmacogn Mag. **13 (**Suppl 4): S828-S833.

Kim SH, Lee HS, Ryu DS, Choi SJ and Lee DS 2011. Antibacterial activity of silver-nanoparticles against *Staphylococcus aureu*s and *Escherichia coli*. Korean J. Microbiol. Biotechnol. **39**: 77-85.

Kumar DA, Palanichamy V and Roopan SM 2014. Green synthesis of silver nanoparticles using *Alternanthera dentata* leaf extract at room temperature and their antimicrobial activity. Spectrochim. Acta A. **127**: 168-171.

Kumara R, Roopan SM, Prabhakarn A, Khanna VG and Chakroborty S 2012. Agricultural waste *Annona squamosa* peel extract: biosynthesis of silver nanoparticles. Spectrochim. Acta A. **90**: 173-176.

Li S, Shen Y, Xie A, Yu X, Qiu L, Zhang L and Zhang Q 2007. Green synthesis of silver nanoparticles using *Capsicum annuum* L. extract. Green Chem. **9**: 852-858.

Matos RA, Cordeiro TS, Samad RE, Vieira ND and Courrol LC 2011. Green synthesis of stable silver nanoparticles using Euphorbia milii latex, Colloid Surface A. **389**: 134-137.

McConnell WP, Novak JP, Brousseau III LC, Fuierer RR, Tenent RC and Feldheim DL 2000. Electronic and optical properties of chemically modified metal nanoparticles and molecularly bridged nanoparticle arrays. J. Phys. Chem. B. **104**: 8925-8930.

Moldovan B, David L, Achim M, Clichici S and Filip GA 2016. A green approach to phytomediated synthesis of silver nanoparticles using *Sambucus nigra* L. fruits extract and their antioxidant activity. J. Mol. Liq. **221**: 271-278.

Moniruzzaman, Shahinuzzaman, Haque A, Khatun R and Yaakob Z 2015. Gas chromatography mass spectrometry analysis and *in vitro* antibacterial activity of essential oil from *Trigonella foenum-graecum*, Asian Pac. J. Trop. Biomed. **5**: 1033-1036.

Mukherjee P, Roy M, Mandal BP, Dey GK, Mukherjee PK, Ghatak J, Tyagi AK and Kale SP 2008. Green synthesis of highly stabilized nanocrysralline silver particles by a non-pathogenic and agriculturally important fungus *T. asperellum.* Nanotechnol. **19**: 103-110.

Mulvaney P 1996. Surface plasmon spectroscopy of nanosized metal particles. Langmuir. **12**: 788-800.

Nakkala JR, Mata R, Gupta AK and Sadras SR 2014. Biological activities of green silver nanoparticles synthesized with *Acorous calamus* rhizome extract. Eur. J. Med. Chem. **85**: 784-794.

Pal S, Tak YK and Song JM 2007. Does the antibacterial activity of silver nanoparticles depend on the shape of the nanoparticle? A study of the gram-negative bacterium *Escherichia col*i. Appl. Environ. Microbiol. **27**: 1712-1720.

Patra JK, Das G and Baek KH 2016. Phyto-mediated biosynthesis of silver nanoparticles using the rind extract of watermelon *(Citrullus lanatus)* under photo-catalyzed condition and investigation of its antibacterial, anticandidal and antioxidant efficacy. J. Photoch. Photobio. B. **161**: 200-210.

Raghunandan D, Mahesh BD, Basavaraja S, Balaji SD, Manjunath SY and Venkataraman A 2011. Microwave-assisted rapid extracellular synthesis of stable bio-functionalized silver nanoparticles from guava *(Psidium guajava)* leaf extract. J. Nanopart. Res. **13**: 2021-2028.

Rai M, Kon K, Ingle A, Duran N, Galdiero S and Galdiero M 2014. Broad-spectrum bioactivities of silver nanoparticles: the emerging trends and future prospects. Appl. Microbiol. Biotechnol. **98**: 1951-1961.

Raja S, Ramesh V and Thivaharan V 2017. Green biosynthesis of silver nanoparticles using *Calliandra haematocephala* leaf extract, their antibacterial activity and hydrogen peroxide sensing capability. Arabian J. Chem. **10**: 253-261.

Rajaram K, Aiswarya DC and Sureshkumar P 2015. Green synthesis of silver nanoparticle using *Tephrosia tinctoria* and its antidiabetic activity. Mater. Lett. **138**: 251-254.

Rastogi L and Arunachalam J 2011. Sunlight based irradiation strategy for rapid green synthesis of highly stable silver nanoparticles using aqueous garlic (*Allium sativum*) extract and their antibacterial potential. Mater. Chem. Phys. **129**: 558-563.

Rycenga M, Cobley CM, Zeng J, Li W, Moran CH, Zhang Q, Qin D and Xia Y 2011. Controlling the Synthesis and Assembly of Silver Nanostructures for Plasmonic Applications, Chem. Rev. **111**: 3669-3712.

S. Acharya, Srichamroen A, Basu S, Ooraikul B and Basu T 2006. Improvement in the nutraceutical properties of fenugreek (*Trigonella foenum-graecum* L.). Songklanakarin J. Sci. Technol. **28**: 1-9.

Sadeghzadeh-Ahari D, Hassandokht MR, Kashi AK, Amri A and Alizadeh KH 2010. Genetic variability of some agronomic traits in the Iranian Fenugreek landraces under drought stress and non-stress conditions. Afr. J. Plant Sci. **4**: 12-20.

Shukla R, Nune KS, Chanda N, Katti K, Mekapothula S, Kulkarni RR, Welshons VW, Kannan R and Katti VK 2008. Soybeans as a phytochemical reservoir for the production and stabilization of biocompatible gold nanoparticles. Small. **4**: 1425-1436.

Sriranjani R, Srinithya B, Vellingiri V, Brindha P, Anthony SP, Sivasubramanian A and Muthuraman MS 2016. Silver nanoparticle synthesis using *Clerodendrum phlomidis* leaf extract and preliminary investigation of its antioxidant and anticancer activities. J. Mol. Liq. **220**: 926–930.

Swamy MK, Sudipta K, Jayanta K and Balasubramanya S 2015. The green synthesis, characterization, and evaluation of the biological activities of silver nanoparticles synthesized from *Leptadenia reticulata* leaf extract. Appl. Nanosci. **5**: 73-81.

Thatoi P, Kerry RG, Gouda S, Das G, Pramanik K, Thatoi H and Patra JK 2016. Photo-mediated green synthesis of silver and zinc oxide nanoparticles using aqueous extracts of two mangrove plant species, *Heritiera fomes* and *Sonneratia apetala* and investigation of their biomedical applications. J. Photochem. Photobiol. B. **163**: 311-318.

Verma A and Mehata MS 2016. Controllable synthesis of silver nanoparticles using Neem leaves and their antimicrobial activity. J. Radiat. Res. Appl. Sci. **9**: 109-115.

Vidhu VK and Philip D 2014. Spectroscopic, microscopic and catalytic properties of silver nanoparticles synthesized using *Saraca indica* flower. Spectrochim. Acta A. **117**: 102-108.

Yahyaei B, Azizian S, Mohammadzadeh A and Pajohi-Alamoti M 2014. Preparation of clay/alumina and clay/alumina/Ag nanoparticle composites for chemical and bacterial treatment of waste water. Chem. Eng. J. **247**: 16-24.

Yang Z, Qian H, Chen H and Anker JN 2010. One-pot hydrothermal synthesis of silver nanowires via citrate reduction. J. Colloid Interface Sci. **352**: 285-291.

Zayed MF, Eisa WH and Shabaka AA 2012. *Malva parviflora* extract assisted green synthesis of silver nanoparticles. Spectrochim. Acta A. **98**: 423-428.

(Manuscript received on 12 February, 2018; revised on 14 November, 2018)